phys. stat. sol. (c) **0**, No. 8, 2956–2960 (2003) / **DOI** 10.1002/pssc.200303848

Formation of Cu_x clusters in Cu/ZnO nanocomposites studied by IR spectroscopy

U. Pal[1,2*], O. Vázquez-Cuchillo[3], A. Bautista-Hernández[2], and J. F. Rivas-Silva[2]

[1] Instituto Mexicano del Petróleo, Programa de Investigación y Desarrollo de Ductos, Eje Central Lázaro Cárdenas 152, Col. San Bartolo Atepehuacan, 07730 Mexico D.F, Mexico
[2] Instituto de Física, Universidad Autónoma de Puebla, Apdo. Postal J-48, Puebla, Pue. 72570, Mexico
[3] Laboratorio de Catálisis Ambiental, IC-BUAP, 14 Sur 6301, Puebla, Pue., 72550 Mexico

Received 30 May 2003, revised 4 August 2003, accepted 11 August 2003
Published online 10 November 2003

PACS: 61.46.+w, 63.22.+m, 78.30.Er, 78.67.Bf

Nanocomposites of Cu/ZnO with different Cu contents were prepared by radio frequency co-sputtering technique. The composite films were annealed at different temperatures in argon atmosphere for 2 hrs. Transmission electron microscopy and x-ray diffraction studies revealed the formation of partially oxidized Cu nanoparticles in ZnO matrix. The size of the Cu nanoparticles depended strongly on the annealing temperature. Infrared spectroscopy study revealed that the nanoparticles consist of an elemental Cu core surrounded by the oxidized copper shell. The elemental core consists of Cu_x clusters. IR spectroscopy and DFT calculation were used to identify the Cu clusters.

1 Introduction

Formation of metal nanoparticles such as Cu, Ag and Au in glass matrix has attracted much attention recently due to their potential applications in non-linear optical devices [1-6]. Several techniques, for example, ion-implantation [2,6,7,8], chemical [9], sol-gel [10] and sputtering [11-13] have been employed by several workers to prepare metal nanocomposites. For the production of nonlinear optical devices, it is important to ensure a certain concentration of such colloidal particles in the matrix. Though a large amount of colloidal particles can be incorporated in the matrix by ion-implantation, the defects created by high energy ions modify their optical properties drastically. On the other hand, by alternate or co-sputtering technique, we can control the amount of dopant easily without modifying the optical properties of the host material. Though, silica or quartz glass have been used vastly as matrix material to prepare colloidal metal particle composites, there are only a few reports on the use of functional matrix material like ZnO for this purpose [11,12,14].

In the present work, an evidence of the formation of Cu nano-clusters in ZnO matrix is presented. Cu/ZnO nanocomposites were grown on quartz glass substrates by r.f. co-sputtering technique and annealed in argon at different temperatures. Transmission Electron Microscopy (TEM), X-ray diffraction and Infra-red (IR) absorption studies revealed that the nanoparticles consist of a metallic Cu core surrounded by a partially oxidized cap layer. Density Function Theory (DFT) in combination with the effective core potentials was used to calculate the optimum geometry of the Cu isomers and their corresponding vibrational frequencies. A comparison of the experimental results with the theoretical calculation revealed that the elemental Cu in the core of the nanoparticles remains mainly in dimer (Cu_2) trimer (Cu_3) and tetramer (Cu_4) cluster forms.

* Corresponding author: e-mail: upal@sirio.ifuap.buap.mx, Fax: +52-22 2295611

2 Experimental

The Cu/ZnO composite films were prepared on well cleaned quartz glass substrates by sputtering of ZnO and Cu wires simultaneously. Different numbers of Cu wires (2 mm length and 0.5 mm of diameter) were placed symmetrically on a ZnO target (50 cm diameter) and sputtered with 200W r.f. power at 20 mTorr Ar pressure. The content of Cu in the films was varied by changing the number of Cu pieces on the ZnO target, keeping the time of sputtering fixed (2 hrs). Depending on the number of Cu pieces, the thickness of the composite films varied from 0.19 μm to 0.22 μm. The as-grown composite films were annealed at different temperatures for 2 hrs in argon atmosphere. A Siemens D5000 X-ray diffractometer with Cuka source was used to record the XRD pattern of the samples. A JEOL 2010 electron microscope was used for obtaining TEM micrographs. A FT-IR Vector 22 spectrometer was used to record the IR absorption spectra of the samples in diffuse mode.

3 Computational details

For the calculation of geometry optimization and vibrational frequencies of Cu clusters, we have used DFT technique in combination with the effective core potentials. This combination has been used currently for the study of metallic clusters with few atoms [15]. The basis set used for the copper atom is the Los Alamos laboratory (LANL) set for effective core potential (ECP) of double-ζ type [16] with relativistic corrections. This pseudopotential consists of small core ECP with 3s and 3p orbitals in the valence space. The functional that we used is the B3PW91 [17], a hybrid functional which define the exchange as a linear combination of Hartree-Fock and gradient-corrected exchange terms [18]. All the calculations were performed using the Gaussian-98 program [19].

Full geometry optimizations were performed via the Berny algorithm in redundant internal coordinates. The thresholds for the convergence were 0.00045 au, 0.0003 au, 0.0018 au and 0.0012 au for the maximum force, root-mean-square (RMS) force, maximum displacement, and RMS displacement, respectively. Once the optimization of cluster geometry is done, the vibrational frequencies were calculated as the second derivative of the energy with respect to the nuclear positions.

4 Results and discussion

Figure 1 shows the typical TEM micrographs of the Cu/ZnO composite films. Formation of nano-clusters in the matrix is clear from the contrast of the micrographs. Most of the nanoparticles were in the range of 3-14 nm in diameter and dispersed homogeneously in the matrix. The average diameter of the nano-clusters increased with the increase of Cu content and also with the annealing temperature [12].

The XRD patterns of the composite films revaled the presence of Cu, both in elemental and oxide form in the composites [12].

To extract the effect of Cu incorporation in the composite films precisely, for the recording of the IR spectra, a quartz substrate with ZnO film on it was used as the reference. For the measurement of IR spectra of the composite films annealed at different temperatures, the ZnO films on quartz substrate annealed at corresponding temperatures were used as the reference. Therefore, the features appeared in the IR spectra are only due to the incorporation of Cu in ZnO.

As the absorption peaks related to the oxides of copper appears in the frequency range 1000-400 cm^{-1} and of elemental Cu in 400-200 cm^{-1}, we divided the full range of measured spectra in two parts: 1000-400 cm^{-1} and 400-200 cm^{-1}.

In figures 2a and 2b, the IR spectra of the as-grown Cu/ZnO composites prepared with different Cu contents are presented for the 1000-400 cm^{-1} and 400-200 cm^{-1} spectral range respectively. For all the samples, we can observe the appearance of two absorption bands at around 530 and 800 cm^{-1} for the 1000-400 cm^{-1} spectral range. There appeared three absorption bands in the low frequency spectral range at around 252, 240 and 226 cm^{-1}. The intensity of the bands increased with the increase of Cu content in the films. Figures 3a and 3b show the IR spectra for the composite films prepared with different Cu contents and annealed at 400^0C for the two spectral ranges. There appeared three absorption bands at around

530, 655 and 800 cm^{-1} for the first spectral range. The absorption band observed at around 655 cm^{-1} was assigned to the symmetric stretching mode of Cu(O2), 2A" with C_{2n} symmetry by several workers [20-23]. The absorption detected at around 530 cm^{-1} was generally assigned to the symmetric stretching vibration of Cu-O bond of the CuOO molecule [24-26]. The last absorption band appeared close to 800 cm^{-1} was assigned to the vibration of Cu-O bond in the CuO_3 molecules [24, 26].

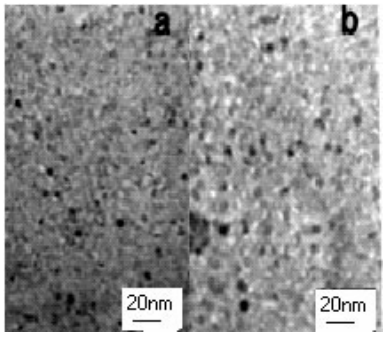

Figure 1. TEM micrographs of the Cu/ZnO composites prepared with 16 pieces of Cu wires a) as-grown and b) annealed at 400^0C.

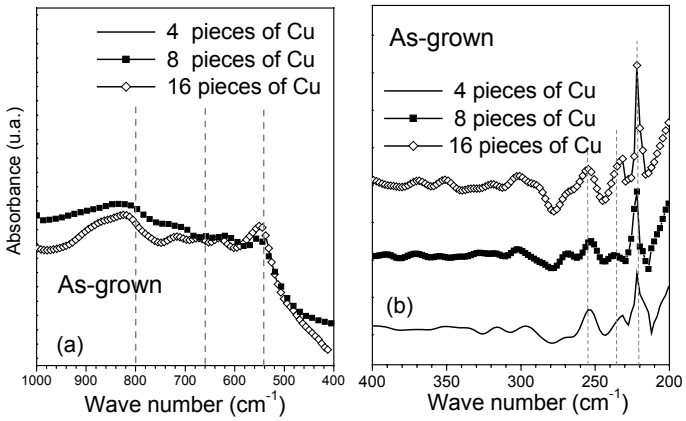

Figure 2. IR spectra of the as-grown composite films prepared with different Cu contents a) for the 1000-400 cm^{-1} and b) 400-200 cm^{-1} spectral ranges.

The peak position of the absorption bands in the 400-200 cm^{-1} spectral range did not change on annealing the sample at higher temperatures. However, on annealing the samples at 400^0C, the relative inten-

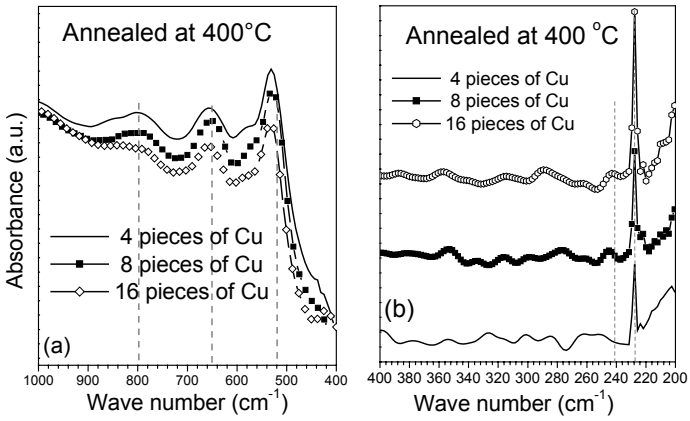

Figure 3. IR spectra of Cu/ZnO nanocomposites prepared with different Cu contents and annealed at 400^0C a) for 1000-400 cm^{-1} and b) for 400-200 cm^{-1} spectral ranges.

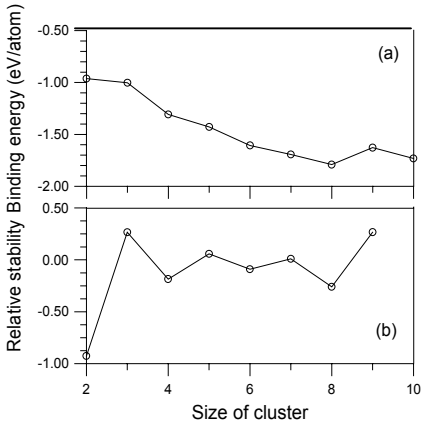

Figure 4. Binding energy (a) and (b) relative stabilities (eV) of Cu clusters calculated by DFT

sity of the 226 cm^{-1} band increased drastically. The first band in this spectral range at about 252 cm^{-1} is assigned to the vibration of Cu_2 linear clusters [27]. The second one appeared at around 240 cm^{-1} is generally assigned to the stretching asymmetric vibration of triangular Cu_3 clusters [28]. However, for the last one appeared at about 226 cm^{-1}, there had been no experimental or theoretical report in the literature. We assigned this band to the vibration of Cu_4 clusters from our theoretical study of vibrational frequencies of Cu_x clusters.

5 Theoretical results

Figure 4 shows the a plot of binding energy versus cluster size (number of Cu atoms). The values of the binding energy for the 2 and 3 atomic clusters are in good agreement with the experimental results [29], and for the other higher size clusters, the values are also in agreement with the reported theoretical results [29]. In the same figure (4b), the relative stability of the Cu clusters is ploted against the number of copper atoms. The relative stability of the Cu clusters was calculated by the relation E=2E(N)-E(N+1)-E(N-1); where, N is the number of Cu atoms in the cluster. We can observe that the clusters formed with N=2,4,6 and 8 are the most stable. In table 1, the most stable spatial geometry and corresponding frequencies of vibration for the Cu clusters for N=2-10 are presented. The highest intensity (more probable) frequencies for each cluster are given in the parentheses.

By comparing our experimental results with the theoretical calculations, we can associate the absorption band appeared at around 252 cm^{-1} to the formation of Cu_2 clusters in the composites. Though the frequency is very close to the calculated frequencies of Cu_5 and Cu_6 clusters, the relative stability of the Cu_2 clusters is higher than the others.

Table 1. Point group and frequencies for the Cu clusters calculated with DFT. The most intense frequencies are given in the parentheses.

Cluster	Point group	Frequencies (cm^{-1})
Cu_2	D_h	(259)
Cu_3	C_{2v}	80, (153), 239
Cu_4	D_2	(220), 58, 112, 149, 255
Cu_5	C_2	(251), 38, 40, 99, 111, 135, 160, 197, 212
Cu_6	D_{3h}	(252), 26, 33, 43, 96, 97, 118, 119, 164, 187, 193, 254
Cu_7	D_{5h}	(208), 60, 105, 106, 119, 123, 127, 146, 147, 153, 155, 209, 223
Cu_8	T_d	(220), 57, 71, 73, 100, 101, 107, 110, 116, 159, 167, 175, 203, 211
Cu_9	C_{3v}	(234), 9, 12, 33, 38, 40, 51, 58, 70, 88, 93, 100, 131, 145, 149, 164, 178, 182, 210, 253, 270
Cu_{10}	D_{4d}	(242), 8, 16, 31, 36, 39, 45, 48, 62, 81, 87, 97, 106, 130, 136, 141, 157, 161, 184, 190, 196, 208, 253, 266

Though our calculation revealed the most intensity frequency for Cu_3 clusters at around 153 cm^{-1}, which is in agreement with the other theoretical works [30]. J. Szeyrbowski et al. [28] have attributed the 240 cm^{-1} frequency to the Cu_3 clusters from their experimental results. It is to be noted that, our theoretical calculation also revealed a frequency at around 239 cm^{-1} but with lower frequency.

The band appeared at around 226 cm^{-1} is very close to the most intensity vibrational frequency for Cu_4 clusters (Table 1). Though the frequency is very close to the most probable frequency for Cu_8 clusters, from the binding energy value in the figure 8a, we can see the formation of Cu_8 cluster is less probable than Cu_4 clusters. Therefore, we assigned our experimental 226 cm^{-1} band to the formation of Cu_4 clusters in the composite films.

6 Conclusions

Incorporation of Cu in ZnO matrix by sputtering resulted the formation of partially oxidized Cu nanoparticles in ZnO matrix. Infra-red absorption and our theoretical calculation using DFT revealed that the nanoparticles consist of an elemental Cu core surrounded by an oxide cap layer. The elemental cores consist of Cu dimer, trimer and tetramer clusters. However, the annealing of the films at 400^0C favored the formation of Cu_4 clusters. A futher theoretical investigation is needed to study the mecanism of this transformation.

Acknowledgements Partial support from VIEP, BUAP (No. II013I02) and CONACyT are gratefully acknowledged.

References

[1] G.I. Stegeman, R.H. Stolen, J. Opt. Soc. B **6**, 652 (1989).
[2] R.F. Haglung Jr., R.H. Magruder III, S.H. Morgan, D.O. Henderson, R.A. Zuhr,L. Yang, R.A. Weller, L. Yang, R.A. Zhur, Nucl. Instrum. Methods B **65**, 405 (1992).
[3] R.H. Magruder III, R.A. Zuhr, R.A. Weeks, Nucl. Instum. and Meth. B **59/60**, 1306 (1991).
[4] R.A. Wood, P.D. Townsend, N.D. Skelland, D.E. Hole, J. Barton, C.N. Afonso, J. Appl. Phys. **74**, 5754 (1993).
[5] N.D. Skelland, J. Sharp, P.D. Townsend, Nucl. Instrum. and Meth. B **90**, 446 (1994).
[6] R.H. Magruder III, R.F. Haglund Jr., L. Yang, J.E. Witting, R. A. Zuhr, J. Appl. Phys. **76**, 708 (1994).
[7] G.W. Arnold, J.A. Border, J. Appl. Phys. **48**, 1488 (1977).
[8] U. Pal, A. Bautista-Hernández, L. Rodríguez-Fernández, J.C. Cheang-Wong, J. Non-Cryst. Sol. **275**, 65 (2000).
[9] M.J. Bolemer, J.W. Hans, P.R. Ashley, J. Opt. Soc. Am. B **7**, 790 (1990).
[10] A. Chatterjee, D. Chakravorty, J. Phys. D: Appl. Phys. **22**, 1386 (1989).
[11] Y. Yoshino, S. Takanezawa, T. Ohmori, Hideki Masuda, Jpn. J. Appl. Phys. **35**, L1512 (1996).
[12] O. Vazquez-Cuchillo, U. Pal, C. Vazquez-Lopez, Solar Energy Mat. & Solar Cells **70**, 369 (2001).
[13] J. Garcia-Serrano, U. Pal, International J. Hydrogen Ener. **28**, 637 (2003).
[14] U. Pal, E. Aguila Almanza, O. Vazquez Cuchillo, N. Koshizaki, T. Sasaki, S. Terauchi, Solar Ener. Mat. & Solar Cells **70**, 363 (2001).
[15] P. B. Balbuena, P.A. Derosa, and J.M. Seminario, J. Phys. Chem. **103**, 2830 (1999).
[16] P. J. Hay, W.R. Wadt, J. Chem. Phys. **82**, 270 (1985); W.R. Wadt, P.J. Hay, J. Chem. Phys. **82**, 284 (1985).
[17] A. D. Becke, J. Chem. Phys. **98**, 5648 (1993); J.P. Perdew, J.A. Chevary, S.H. Vosko, K.A. Jackson, M.R. Pederson, D.J. Singh, C. Fiolhais, Phys. Rev. B **46**, 6671 (1992).
[18] J. P. Perdew, Y. Wang, Phys. Rev. B **45**, 13244 (1992).
[19] Gaussian 98, Revision A.9, M.J. Frisch et al. Gaussian, Inc., Pittsburgh PA, 1998.
[20]V. E. Bondybey, J.H. English, J. Phys. Chem. **88**, 2247 (1984).
[21] W. Hongbin, R. Sunil, and W. Lai-Sheng, J. Chem. Phys. **101**, 3898 (1994).
[22] W. Hongbin, S.R. Desai, and W. Lai-Sheng, J. Phys. Chem.A **101**, 2103 (1997).
[23] D.E. Tevault, J. Chem. Phys. **76**, 2859 (1982).
[24] G.V. Chertihin, L. Andrews, C.W. Bauschlicher, Jr., J. Phys. Chem. A. **101**, 4026 (1997).
[25] K.P. Muthe, J.C. Vyas, N.S. Narag, D.K. Aswal, S.K. Gupta, D. Bhattacharya, R. Pinto, S.C. Sabharawal, Thin Solid Films **324**, 37 (1998).
[26] D.E. Tevault, R.C. Mowery, R.A. Demarco, R.R. Smardzewsky, J. Chem. Phys. **34**, 244 (1981).
[27] H. Hongbin, R. Sunil and W. Lai-Sheng, J. Chem. Phys. **101**, 3898 (1994).
[28] J. Szeyrbowski and A. Czapla, Thin Solid Flims **46**, 127 (1977).
[29] A. J. Bhattacharyya, A. Mookerjee and A. K. Bhattacharyya, arXiv:cond-mat/0001285 v1 20 Jan 2000.
[30] P. Calaminici, A. M. Koster, N. Russo, D. R. Salahub, J. Chem. Phys. **105**, 9546 (1996).